URSI GASS 2023, Sapporo, Japan, 19 – 26 August 2023

Vehicle Shadowing Modeling for Deterministic Channel Emulator and Electromagnetic Simulation-Based Validation

Siraphop Saisa-ard*[(1)], Nopphon Keerativoranan[(1)], and Jun-ichi Takada[(1)]
(1) Tokyo Institute of Technology, Tokyo, Japan;
e-mail: saisa.s.aa@m.titech.ac.jp; nopphon.keerativoranan@ap.ide.titech.ac.jp; takada@tse.ens.titech.ac.jp

Abstract

Due to the development of a deterministic channel emulator for virtual communication system verification, a simple and realistic model for shadowing gain prediction caused by moving objects, e.g., vehicles, is necessary. In this work, a vehicle shadowing model based on knife-edge diffraction model which uses the shortest diffraction path is presented. The model is verified by using the shadowing gain calculated from the electromagnetic simulation result of a vehicle frame and a PEC cuboid of its size at 700 MHz-band. The slow-fading component result shows that the model is able to predict the gain well during the shallow-shadow region which is of more interest for channel modeling.

1 Introduction

Due to the advancement of intelligent transport system (ITS) which includes many safety-critical applications such as autonomous vehicles, a channel emulator with high level of realism is necessary for the communication system verification prior to the deployment. The vehicular channel in ITS is characterized as highly nonstationary and the communication links are frequently shadowed by other vehicles in the traffic [1], due to the movement of transmitter (Tx), receiver (Rx) and other vehicles. Shadowing effect is even more evident in the vehicle-to-vehicle (V2V) communication due to the low-profile antennas.

In order to develop a channel emulator for ITS, the shadowing effects caused by the moving vehicles must be predicted. There are 3 main approaches for vehicular channel modeling and the shadowing in it [1]. The geometry-based stochastic model such as 3GPP [2] models vehicle shadowing by blockage B model which assume a fixed-size rectangular obstacle with random mobility pattern. The deterministic model such as a snapshot-by-snapshot full ray-tracing (RT) simulation technique [3] uses a set of dominant paths from the entire environment to simulate the channel. Lastly, the simplified geometry-based model uses simplified geometrical information with insights from the deterministic model or measurement, such as GEMV model [4] that classifies the link types into line-of-sight (LoS) and non-line-of-sight (NLoS), and model them separately.

In consideration for the development of the emulator in ITS scenario, the underlying channel model must be site-specific, so the stochastic model is not sufficient [2]. However, the emulator must be able to run in near real-time and large-scale, so the deterministic model is not feasible. Therefore, the geometry-based model that uses the pre-processed RT simulation [5] is developed to fulfill the site-specific and near real-time requirements of the emulator.

Nevertheless, there is still the research challenge regarding the modeling of the effect of moving objects. To keep the channel model simple, only the shadowing on the pre-calculated RT paths is considered. Hence, the objective of this work is to develop a simple vehicle shadowing gain prediction model and validate it deterministically by using electromagnetic (EM) simulation. The frequency band under consideration is 700 MHz-band as it is allocated for the vehicular communication in Japan [6].

2 Proposed Model

The vehicles in this work are modeled as cuboids with PEC material hovering above the PEC ground with the same distance as if there were wheels. The small components, e.g., side mirror, wheel, and headlight, are not considered. As the scope of this work is limited to shadowing, only a single pair of Tx and Rx is considered, so it is assumed that vehicles do not generate additional reflection paths. The originalities of this work include:

1. The shadowing condition determination method which is an extension of 60% first Fresnel zone in [4] to consider the obstructed line-of-sight (OLoS) case.
2. The single dominant path knife-edge diffraction (KED) model which takes the 3D geometry of the object into account in a simple manner.
3. The validation method that is based on EM simulation which allows the mechanism of the shadowing to be explained.

2.1 Shadowing condition determination

First Fresnel zone is the area surrounding the optical path between the Tx and Rx, with the size proportional to the wavelength λ. In this work, three shadowing conditions are defined: LoS, OLoS, and NLoS as depicted in Fig. 1. The LoS condition is the case where the whole first Fresnel zone is clear of obstruction. The OLoS condition is defined as the obstruction of more than 60% of the first Fresnel zone by any part of the cuboid, but the optical path is clear. The NLoS condition is as the obstruction of the optical path.

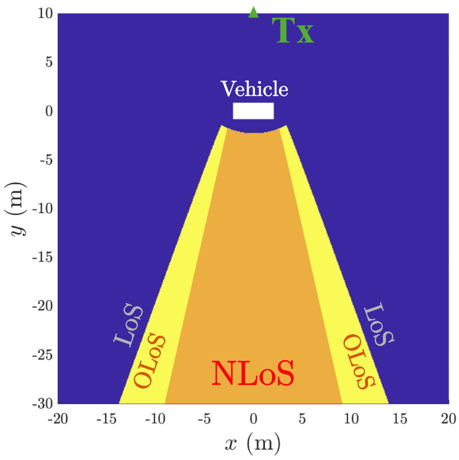

Figure 1. Illustration of LoS, OLoS and NLoS caused by a shadowing cuboid from top view

To allow fast calculation, the vehicle is assumed to cause OLoS condition when its bounding sphere touches 60% of the first Fresnel zone which also includes the case when the sphere contains Tx or Rx inside. Furthermore, the link is in NLoS if the cuboid faces of the vehicle intersect the optical path.

2.2 Diffraction model

Under OLoS or NLoS conditions, the diffraction point (DP) is calculated as the point on the cuboid that minimizes the Tx-DP-Rx distance if there is a single interaction path, i.e., a cuboid edge is visible from both Tx and Rx. If no single interaction path exists, DP is calculated by using the principle of Bullington's method to find the point outside cuboid which minimizes the Tx-DP-Rx distance without entering the cuboid. The DPs for the single and double interaction path are illustrated in Fig. 2 and Fig. 3 respectively.

The model adopts the KED model to calculate the shadowing gain $|G(\nu)|_{\mathrm{dB}}$. The approximated formula [7] is used as it provides reasonable accuracy in the shadowed region as,

$$|G(\nu)|_{\mathrm{dB}} = \begin{cases} -6.9 - 20\log(\sqrt{(\nu-0.1)^2+1}+\nu-0.1), & \text{if } \nu > -0.78 \\ 0 & \text{otherwise,} \end{cases} \quad (1)$$

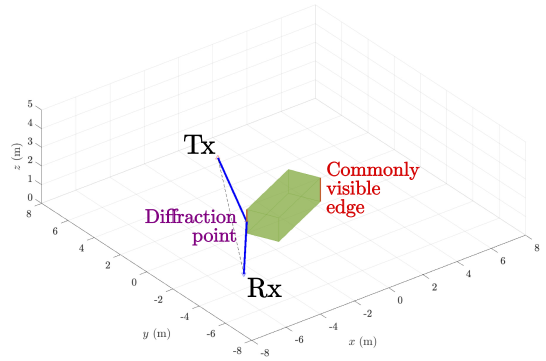

Figure 2. The diffraction point with single interaction path

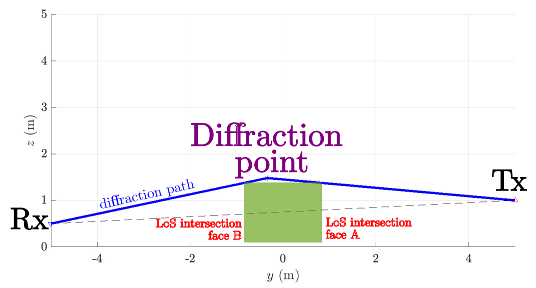

Figure 3. The diffraction point with double interaction path

where $\nu = h\sqrt{2/\lambda F_e}$ is the KED parameter, h is the distance from the DP to the optical path where it positive in NLoS and negative in OLoS, $F_e = (1/d_1 + 1/d_2)^{-1}$ is the equivalent focal length, d_1 and d_2 are the distance from Tx and Rx to the DP respectively. The physical implication of the model is that the diffraction path propagates over the knife-edge which is proportional to the optical path at the diffraction point location. Thus, the model is valid when the knife-edge resembles the physical edge of the cuboid, i.e., the object is not too small compared to the first Fresnel zone. The model also assumes that the Tx-DP-Rx distance of the case with single interaction is always shorter than the case with double interaction path.

3 Model Validation

The proposed model has 2 major assumptions that need to be verified. Firstly, the vehicle is modeled as a PEC cuboid which ignores the complex geometry of the vehicle, especially the window. Moreover, the design of modern vehicles comprises of curved edges, the effect of surface creeping wave may be noticeable especially because the vehicular communication is usually short range. Secondly, the diffraction over a PEC cuboid is approximated by a single diffraction path using the KED model, so the effect of thickness, which can be treated in some cases by UTD, and the phasic effect of multipaths or Fresnel diffraction are neglected.

3.1 Electromagnetic simulation

To verify both assumptions, the scattered electric near-field of a vehicle frame and a PEC cuboid is simulated using the integral equation solver in the commercial software Ansys HFSS [8]. The object is placed at the origin facing toward $+x$ direction, and the Tx is positioned 10 m away at 1 m height. The electric field is observed along the trajectory depicted in Fig. 4. The ground is modeled as an infinite PEC plane at $z = 0$. Detailed simulation parameters are presented in Table 1.

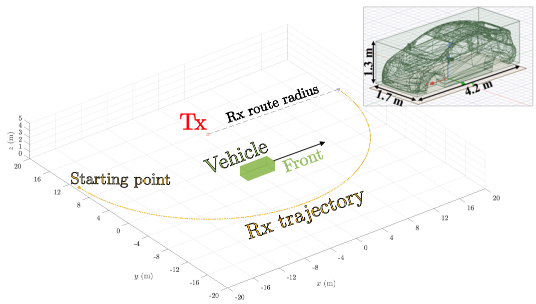

Figure 4. Simulation scenario and the vehicle geometry

Table 1. Parameters of the simulation scenario

Parameters	Values
Radio system	
Frequency	760 MHz
Antenna	Vertical electric Hertzian dipole
Tx location	(0, 10, 1) m
Rx route radius	20 m
Rx height	0.5 m
Vehicle geometry	
Model	Toyota Prius
Size	$4.181 \times 1.678 \times 1.275$ m
Center location	(0, 0, 0) m
Hover height	0.1 m

The shadowing gain is calculated from the simulated electric field by,

$$|G(v)|_{\mathrm{dB}} = -20\log_{10}\left|\frac{E_{\mathrm{s}}+E_{\mathrm{i}}}{E_{\mathrm{i}}}\right|, \tag{2}$$

where E_{s} is the scattered field simulated by HFSS, and E_{i} is the incident field by using the formula for ideal dipole. Since the observation trajectory is a semi-circle around Tx with constant elevation angle, E_{i} is constant.

3.2 Simulation Results

The shadowing gain obtained from the EM simulation for the vehicle frame and PEC cuboid are plotted together with the result using the proposed KED model in Fig. 5. Overall, the model shows a general agreement with the EM simulation of both vehicle frame and PEC cuboid, in particular in the shallow-shadow (transition) which is considered to be more important than the deep shadow because it still contributes to the communication system. The model shows an unexpected drops of approximately 3 dB in the deep shadow region which are due to the shadowing condition transition. The fast-fading components can be vividly observed for both the vehicle frame and PEC cuboid in the LoS region with the maximum magnitude around 2 dB. Symmetric sharp drops as much as -17 dB are present for the PEC cuboid due to destructive interference between the side diffraction and over-the-roof diffractions. Similarly, small peaks up to -6 dB can be explained as the constructive interferences of 2 sides and over-the-roof diffractions. On the other hands, the shadowing gain from the vehicle frame does not show as much effect of the interference.

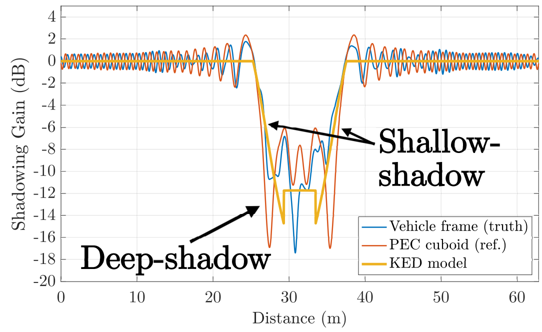

Figure 5. Simulated shadowing gain

3.3 Slow-fading components

The slow-fading components of the shadowing gain can be calculated by applying the windowed average. The result using 10λ rectangular window along the Rx trajectory is presented in Fig. 6. As the scope of this work is limited to shadowing, only the obstructed first Fresnel zone region is considered which is highlighted by the solid lines. By comparing the slow-fading components, the agreement between the model and the cuboid in the shallow shadow region becomes clearer, and the difference to the vehicle frame in the right half (car front) becomes more distinct. This can be explained as the effect of the slanted hood and the holes through the windshield and the window. In deep shadow region, the model underestimates the gain by 1.5 dB which is expected to be due to the single dominant path approximation. In contrast, the PEC cuboid overestimates the gain by 2.5 dB which is caused by the constructive interference from the perfect symmetry of both the vehicle geometry and environment which is a rare occurrence in real world.

3.4 Fast-fading components

Even though shadowing is considered a large-scale phenomenon, its fast-fading may still have some effect on the overall channel statistics. The fast-fading components can be calculated as the deviation of the original gain from its local mean (slow-fading) in dB. The empirical cumulative density function (ECDF) of the deviation is presented in Fig. 7, and deviation itself is depicted in the small figure.

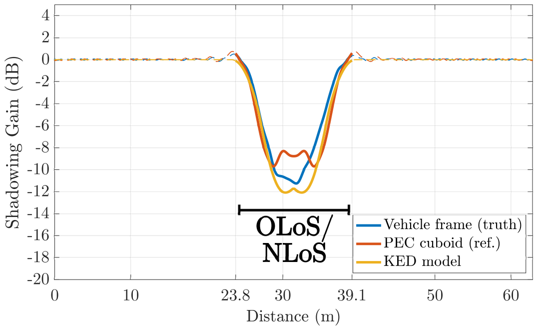

Figure 6. Slow-fading components using moving average with 10λ window

The ECDF of the model shows that it the gain has little fast-fading components as the maximum absolute deviation is -3.3 dB while they are -6.5 dB and -9.2 dB for the vehicle frame and PEC cuboid. Therefore, it can be observed that even though the proposed model can acceptably predict the slow-fading, it fails to reproduce any small-fading as expected because it does not consider phase which causes the variations in small-scale. In addition, it is observed that the small-scale variation of the vehicle frame is more random than the PEC cuboid.

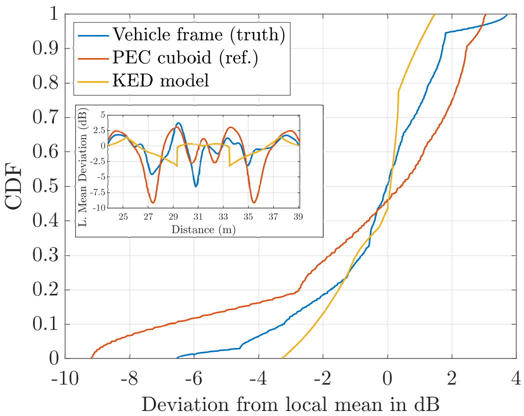

Figure 7. Slow-fading components using moving average with 10λ window

4 Conclusion

The single dominant path KED model and the method to determine the shadowing condition are developed to predict the vehicle shadowing gain at 760 MHz-band. The comparison between the simulated gain with those obtained from the EM simulation shows that the model can acceptably be used to emulate the shadowing in the wireless channel emulator as the fast-fading components can be modeled separately. In addition, the slow-fading result shows that it is advisable to consider the slanted front of the vehicle instead of an ordinary cuboid. Additional simulation in other scenarios may be required to support the conclusion with greater certainty.

Acknowledgements

This research is supported by the Ministry of Internal Affairs and Communications of Japan under the contract "R&D for the realization of high-precision radio wave emulator in cyberspace" (JPJ000254).

References

[1] W. Viriyasitavat, M. Boban, H. M. Tsai and A. Vasilakos, "Vehicular Communications: Survey and Challenges of Channel and Propagation Models," in *IEEE Vehicular Technology Magazine*, vol. 10, no. 2, pp. 55-66, June 2015, doi: 10.1109/MVT.2015.2410341.

[2] 3GPP, "Study on channel model for frequencies from 0.5 to 100 GHz," Tech. Rep., 2019, TR 38.901, ver. 16.1.0

[3] J. Maurer, T. Fugen, T. Schafer and W. Wiesbeck, "A new inter-vehicle communications (IVC) channel model," *IEEE 60th Vehicular Technology Conference*, 2004. VTC2004-Fall. 2004, Los Angeles, CA, USA, 2004, pp. 9-13 Vol. 1, doi: 10.1109/VETECF.2004.1399905.

[4] M. Boban, J. Barros and O. K. Tonguz, "Geometry-Based Vehicle-to-Vehicle Channel Modeling for Large-Scale Simulation," in *IEEE Transactions on Vehicular Technology*, vol. 63, no. 9, pp. 4146-4164, Nov. 2014, doi: 10.1109/TVT.2014.2317803.

[5] N. Keerativoranan and J. Takada, "Site-Level Deterministic Channel Emulator: Grid-based Architecture and Continuous Channel Emulation Technique," *2022 16th European Conference on Antennas and Propagation (EuCAP)*, Madrid, Spain, 2022, pp. 1-5, doi: 10.23919/EuCAP53622.2022.9769688.

[6] ARIB, "700 MHz Band Intelligent Transport Systems," Tech. Rep., 2017, ARIB STD-T109, ver. 1.3

[7] ITU-R, "Propagation by diffraction," 2019, RECOMMENDATION ITU-R P.526, ver. 15

[8] Ansys Electronics Premium HFSS. Release 22.1, ANSYS, Inc